DEPARTMENT OF DEFENCE
DEFENCE SCIENCE & TECHNOLOGY ORGANISATION
DSTO

DSTO

Extra Low Frequency (ELF) Coils for the Marine Environment Data Acquisition System (MEDAS)

David Clarke

DSTO-TR-0876

Extra Low Frequency (ELF) Coils for the Marine Environment Data Acquisition System (MEDAS)

David Clarke

Maritime Operations Division
Aeronautical and Maritime Research Laboratory

DSTO-TR-0876

ABSTRACT

Three Extra Low Frequency (ELF) coils for measuring low frequency magnetic signatures were designed and built for use with the Marine Environment Data Acquisition System (MEDAS) concept demonstrator. This report details the tests conducted to determine the performance of these coils. A circuit model of the ELF coils is developed so the output of the coils may be related to the incident magnetic field. The values for the resistance, inductance and capacitance are measured and calculated from details of the construction. The effect of incorporating a calibration winding for checking the in-situ underwater response of the ELF coils is also examined.

RELEASE LIMITATION

Approved for public release

DEPARTMENT OF DEFENCE
DEFENCE SCIENCE & TECHNOLOGY ORGANISATION
DSTO

Published by

DSTO Aeronautical and Maritime Research Laboratory
PO Box 4331
Melbourne Victoria 3001 Australia

Telephone: (03) 9626 7000
Fax: (03) 9626 7999

AR-011-084
September 1999

APPROVED FOR PUBLIC RELEASE

Extra Low Frequency (ELF) Coils for the Marine Environment Data Acquisition System (MEDAS)

Executive Summary

Extra Low Frequency (ELF) coils are used for measuring the low frequency magnetic signature of ships and submarines. This report details the testing and theoretical calculations used in determining the performance of the three ELF coils used for measuring low frequency (1-600 Hz) magnetic signatures in the Marine Environment Data Acquisition System (MEDAS). Each coil consists of two windings on a polypropylene former. The primary winding of 1632 turns for detecting incident signals and an excitation winding of 6 turns used to check the performance of the primary winding when MEDAS is deployed.

The magnetic test facility (also called the uniform magnetic volume) at the Underwater Systems Division (now Maritime Operations Division Maribyrnong) was used to apply an incident magnetic signal of a set frequency to each ELF coil. The output was recorded and simple signal processing was used to determine the amplitude and phase shift. This procedure was repeated over the bandwidth to determine the frequency response of the ELF coils. A similar process was repeated with the excitation winding so the frequency response of the primary winding when stimulated by the excitation winding was known. The sensitivity of the coils was measured to be approximately 12.9 mV/(μT.Hz) at frequencies below 100 Hz.

A circuit model of the ELF coils was developed and the values for the components in the circuit model were measured. Methods were also developed to calculate the values of the circuit model components to facilitate any future design of ELF coils. The results of the measured frequency response were used to confirm the circuit model and circuit values of the ELF coils.

In MEDAS the signal from the ELF coils was converted from the time domain into the frequency domain. Once the data was in the frequency domain calculations using the verified circuit model of the ELF coils were then used to determine the amplitude of the incident signal at specified frequencies.

MEDAS was developed and deployed as a concept demonstrator and is no longer in service. The ELF coils used in MEDAS have been transferred to the Maritime Operations Division (Sydney) for use in continuing research in this field.

Contents

1. Introduction

The presence of a vessel may be detected by its magnetic signature. Extra Low Frequency (ELF) coils are used for measuring the low frequency magnetic signature of ships and submarines. Some of the sources of the ELF signatures on the vessels [1] include

i) electrical power generation equipment,
ii) the current in the electrical wiring,
iii) the rotating propeller and propeller shaft.

The ELF coils analysed in this report were built as part of a multisensor concept demonstrator package called MEDAS (Marine Environment Data Acquisition System) for the Royal Australian Navy. In order to interpret the output from each coil it is necessary to determine the frequency response of each coil. Once the frequency response of each coil is known it is possible to determine the ELF magnetic signature of a vessel from the output of these coils.

A straight curve for the frequency response across the bandwidth is desirable as it simplifies the processing of the output and improves coil sensitivity at high frequencies. This response occurs when the resonance frequency is well beyond the bandwidth of interest. For the ELF coils used with MEDAS the bandwidth of interest was 1 - 600 Hz. For the ELF coils used in MEDAS the sensitivity was approximately 12.9 mV/(μT.Hz) up to 100 Hz, increasing to around 13.6 mV/(μT.Hz) at 600 Hz. The resonance frequency for the ELF coils when connected to an impedance equivalent to the input impedance of the MEDAS circuitry was measured as approximately 2150 Hz.

Further analysis was carried out in order to optimise the use of these coils and facilitate the design and construction of future coils. This analysis examined the capacitances present in the coil and methods were developed to predict the magnitude of these capacitances. The inductance of the windings within the ELF coils was also calculated. Once the capacitance, inductance and resistance of an ELF coil is known the frequency response of the ELF coil may be determined. As part of this analysis the optimum positioning of the excitation winding was also examined.

2. Construction of ELF Coils

The construction of the ELF coils is sketched in Figure 1. The dimensions of the ELF coils used in MEDAS are very similar to the coils designed by Vrbancich et al [2][3] although the former is constructed in a different manner. Vrbancich [3] acknowledges that he adopted the construction techniques suggested by Holtham [4] and Wesley [5]. The ELF coils used in MEDAS are comprised of two sets of windings on a polypropylene former. The polypropylene former has an inside diameter of 1.15m, an outside diameter of 1.302m and a width of 80mm. Inset into this ring is six rectangular slots 6mm wide, 27mm deep and separated by 4mm.

The excitation winding of six turns was placed at the bottom of the sixth slot. The primary winding of 1632 turns was evenly divided between the six grooves, 8 windings across and 34 windings deep (Figure 1). The purpose of the excitation winding is to provide a known excitation to the primary winding so the correct operation of the ELF Coil(s) and the associated electronics maybe verified.

Three ELF coils were assembled, two of the coils closely fitted the above specifications for the number of windings, the third coil however was short approximately thirty five turns. The three ELF coils were designated Coil A, Coil B and Coil C. Coil B does not closely fit the winding specifications.

Once the winding of the ELF coils was completed and their sensitivities determined the coils were sealed to prevent seawater from entering. It is important to prevent any seawater entering the ELF coils as seawater has a high permittivity, thus the presence of seawater in the coil would increase the capacitance of the coil. Seawater inside the ELF coil may also cause corrosion problems or short circuit part or the entire coil.

In operation the three coils are orientated perpendicular to one another. One cable goes from each coil to a junction box, from the junction box one cable leads to the processor unit. At the processor unit the signal is amplified then digitised.

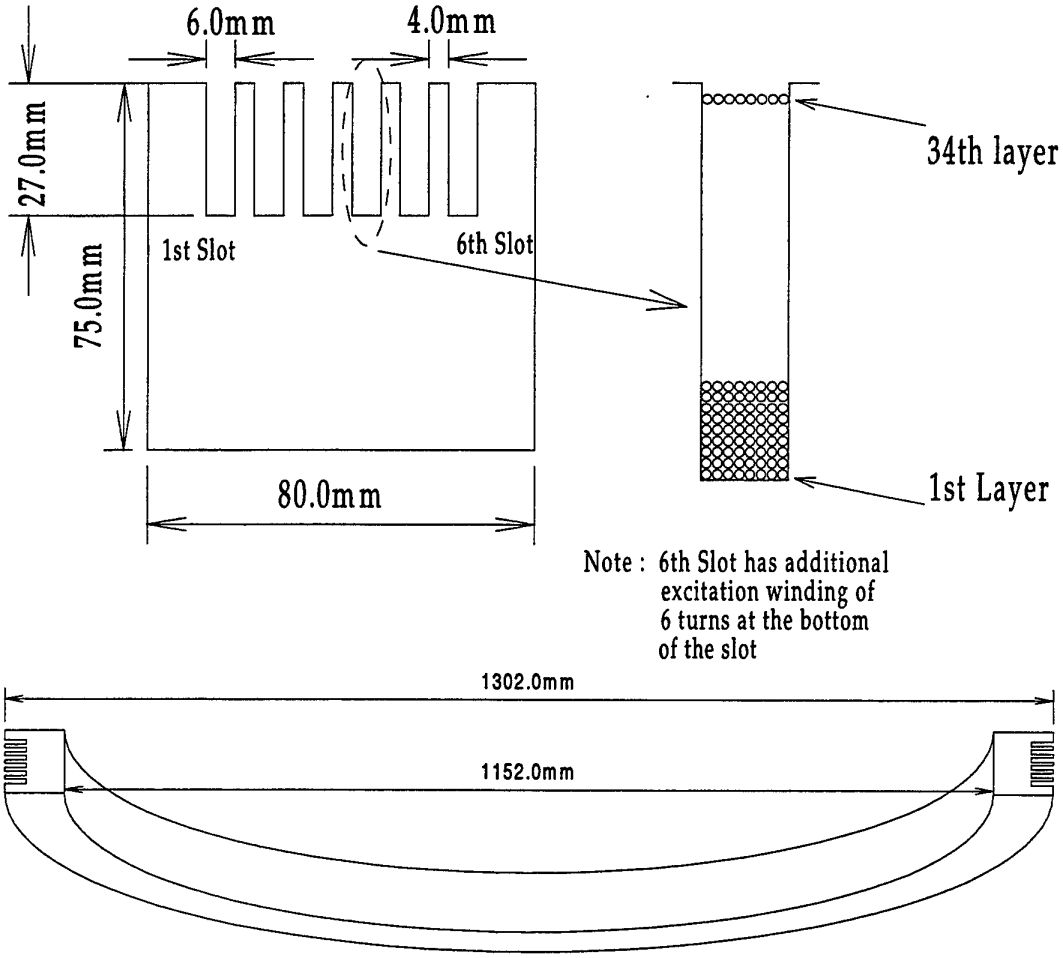

Figure 1. - Construction of MEDAS ELF Coils

3. Experimental Measurements

The ELF coils with their associated cabling were tested in the DSTO Magnetic Test Facility at Maribyrnong. This facility is usually used to generate a magnetic field that is uniform to within 1% over a working region of 1 metre diameter by 6 m long[1]. As the MEDAS ELF coils are larger than the normal working area of the Magnetic Test Facility the magnetic flux density through a 1.3 m diameter section of the Magnetic

[1] No published reference available

Test Facility was measured for a range of frequencies. The value obtained from these measurements were used to determine the magnetic field incident on the ELF coils under test and only differed from the standard calibration factor for the Magnetic Test Facility by 4 %. The reduction in homogeneity due to working outside the standard working region of the Magnetic Test facility is not important as long as the total magnetic flux passing through each ELF Coil is known. Each ELF coil was measured individually.

The frequency response of the primary winding was determined by exciting the coils of the Magnetic Test Facility with a sinusoidal wave over the bandwidth 1 Hz to 1 kHz and monitoring the voltage induced across the ELF primary winding.

The Magnetic Test Facility was excited by a sine wave of frequency ω producing a magnetic field of amplitude B_0. The output from the ELF coil, $V(w)$ may be fully described as

$$V(\omega) = A \sin \omega + C \cos \omega + N(\omega) \quad (1)$$

where A and C are constants and $N(w)$ accounts for the noise in the system and the environment, mainly 50 Hz and its harmonics and includes all frequency components not equal to ω. The value of A can be determined by multiplying the output $V(w)$ with $\sin\omega$ and integrating the result over an integer number of periods. Similarly by multiplying the output $V(w)$ by $\cos\omega$ and integrating over an integer number of periods the value of C may be obtained. With this information the phase shift P_S and sensitivity of the primary winding S_P can be determined from Equations 2 and 3 respectively.

$$P_S = \tan^{-1}\left(C/A\right) \quad (2)$$

$$S_P = \sqrt{\left(A^2 + C^2\right)} \quad (3)$$

The output $V(w)$ was a segment of approximately twenty periods of ω that had been averaged sixty four times in order to increase the signal to noise ratio. As the voltage induced across the winding is approximately proportional to the frequency it was necessary to amplify the signal by a hundred for the lower frequencies, less than 40 Hz, before digitisation. The frequency response of the primary coil and the associated electronics is shown in Figure 2.

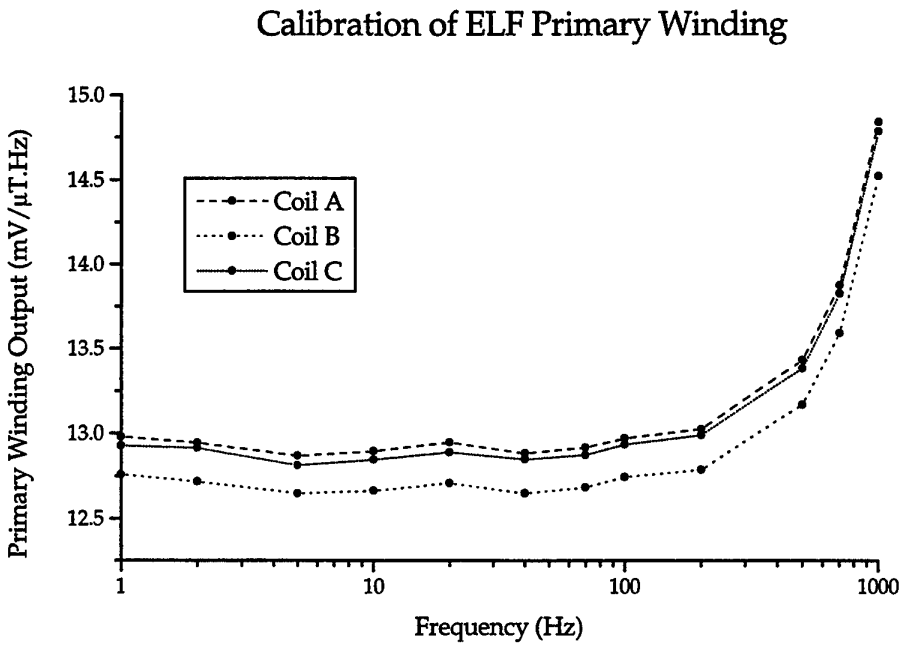

Figure 2. - Calibration of ELF Primary Winding

The performance of the excitation winding on the ELF coils was tested in a similar manner. Instead of using the uniform magnetic region to induce a voltage in the primary winding a current was passed through the excitation windings to induce a voltage on the primary winding of the ELF coil. The output from the primary winding was measured in the same manner. Figure 3 displays the frequency response of the primary coil when excited by the excitation winding. The shape of the frequency response curve of the primary when excited by an incident field and the excitation winding are compared in Figure 4.

The values for the calibration of the ELF coils obtained from Figure 2 will be used to develop a calibration curve for use in MEDAS. An appropriate form of supplying the calibration curve would incorporate the circuit (or effective) components. This would not only supply a calibration curve that represents the coils performance but also allow for changes in the output resistor to be easily incorporated.

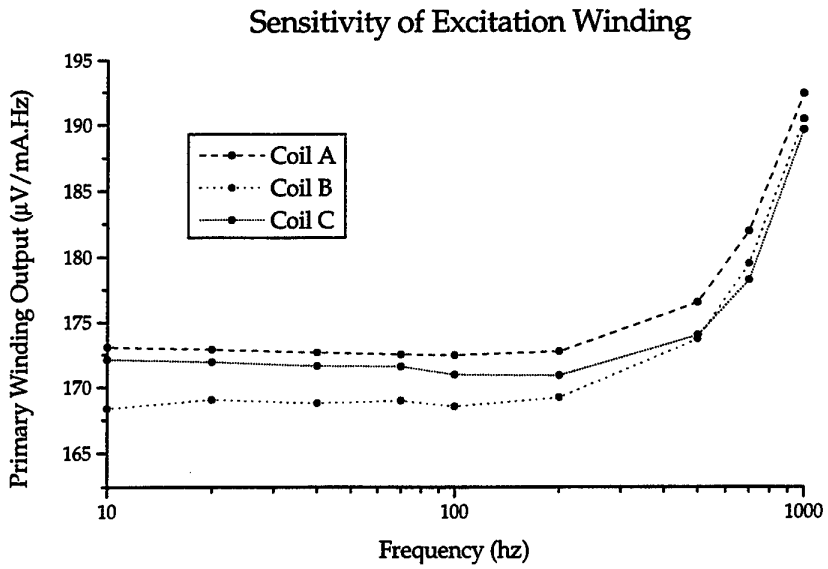

Figure 3 - Output of ELF Primary winding due to current flow in Excitation Winding

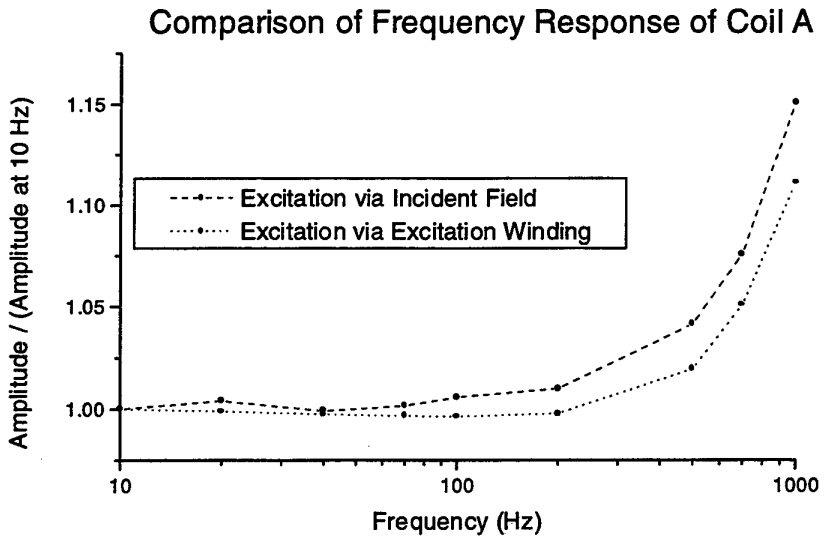

Figure 4 a) - Comparison of the frequency response measured using an incident field and the excitation winding to stimulate the primary winding of ELF Coil A.

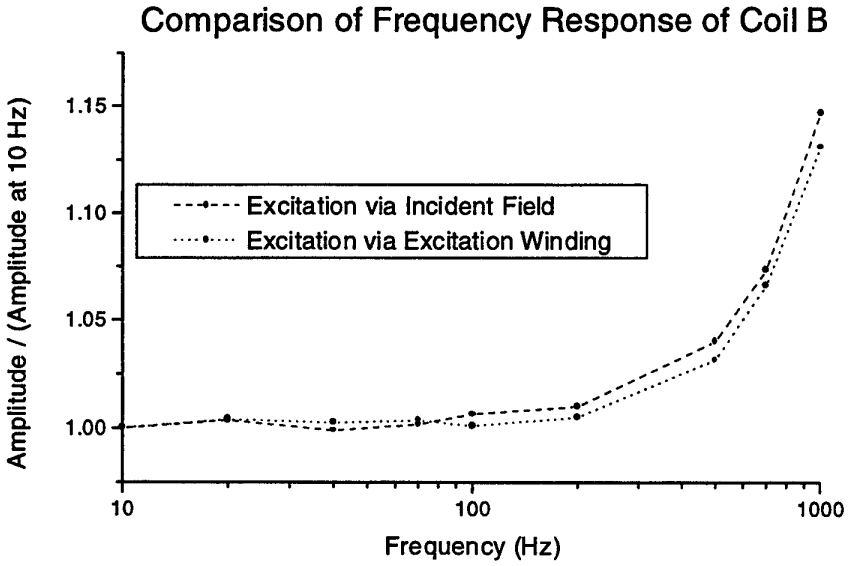

Figure 4 b) - Comparison of the frequency response measured using an incident field and the excitation winding to stimulate the primary winding of ELF Coil B.

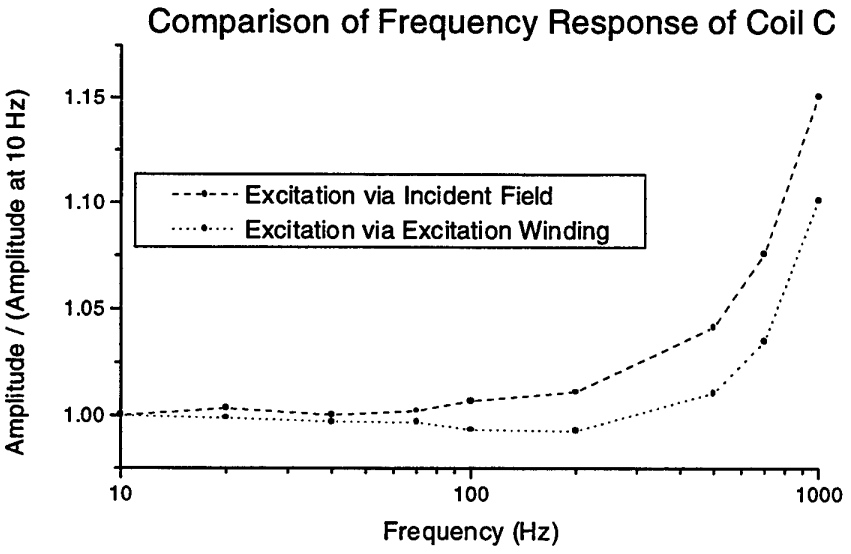

Figure 4 c) - Comparison of the frequency response measured using an incident field and the excitation winding to stimulate the primary winding of ELF Coil C.

It is evident from Figure 4 that the curve shape generated using the incident field differs a little from the curve shape generated using the excitation winding. It appears that the resonnace frequency may have increased when the excitation winding is used. The apparent difference may be exagerated as the experimental error will have been increased by dividing the curves by their value at 10 Hz in order to compare curve shapes. The only difference in the set up of the ELF coil is that a current is now passing through the excitation winding. As the resistance of the excitation winding is very low the potential difference across the interwinding capacitance however should for all practical purposes remain unchanged.

The largest difference in shape occurs for coil A and C, which have an interwinding capacitance 30 % larger than coil B (section 7). The author however doesn't believe that this would explain the apparent increase in resonance frequency due to the small change in the potential difference across the interwinding capacitance. As the purpose of the excitation winding is to provide a magnetic field to verify the correct functioning of the primary winding and the associated electronics, not to calibrate the coil this difference was not further investigated.

4. Circuit Model

The primary winding of the device was modelled as an LCR circuit as shown in Figure 5 with the voltage source V_{pri}, where V_{pri} is the voltage induced in the winding by the external field. Faraday's law of electromagnetic induction can be used to calculate V_{pri}.

$$V_{pri} = -N A B_0 \omega \cos(\omega t) \qquad (4)$$

where N is the number of coils on the primary winding, A is the average area surrounded by each coil and t is time.

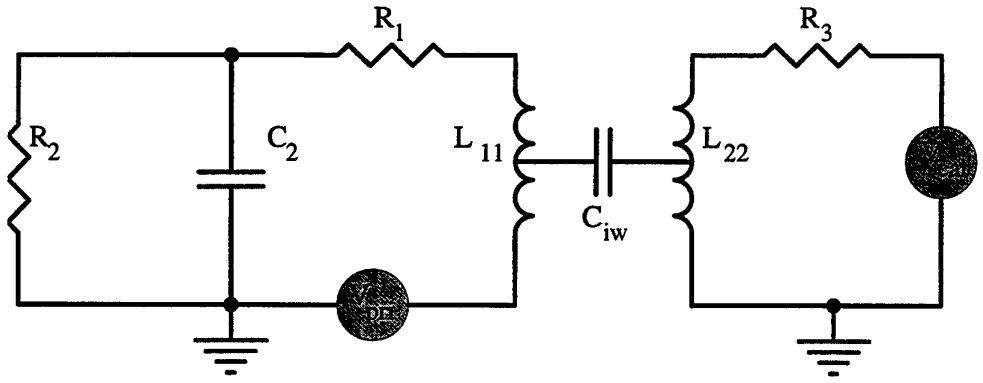

Figure 5 - Circuit Model of ELF Coil

In Figure 5 R_1 is the resistance of the primary winding, R_2 is the output resistor, R_3 is the resistance of the calibration winding, C_2, is the total capacitance of the primary winding, C_{iw} is the interwinding capacitance between the primary and calibration windings, L_{11} is the inductance of the primary winding and L_{22} is the inductance of the calibration winding. The voltage induced in the primary winding is represented by V_{pri} and the voltage used to excite the calibration winding is V_{cal}. The impedance Z_t experienced by the induced voltage can be determined from Figure 5.

$$Z_t = R_1 + \frac{R_2}{1+(\omega R_2 C_2)^2} + j\left(\omega L_{11} - \frac{R_2}{1+(\omega R_2 C_2)^2}\right) \qquad (5)$$

Using equation 5 the current I_1 flowing through the inductor L_{11} due to the voltage V_{pri} may be determined.

$$I_1 = \frac{V_{pri}}{Z_t} \qquad (6)$$

The measured output from the primary winding is the voltage across R_2, V_{R2}. Analysis of the circuit in Figure 5 shows that

$$V_{R2} = \frac{(X - jY) R_2 V_{pri}}{X^2 + Y^2} \qquad (7)$$

where $X = R_1 + R_2 - \omega^2 L_{11} R_2 C_2$ and $Y = \omega L_{11} + \omega R_1 R_2 C_2$. The phase shift θ from V_{pri} to V_{R2} is determined by

$$\theta = \tan^{-1}\left(\frac{Y}{X}\right) \qquad (8)$$

In order to use Equations 7 and 8 the values of the various components must be determined. These values can be measured. However if these values could be predicted the design of these coils would be facilitated. The resistance of the primary R1 is calculated in section 5. In sections 6 and 7 methods are developed to calculate the inductances and capacitances present in the ELF coils.

5. Resistance

The resistance of the primary winding R_1 (Figure 5) may be calculated as the diameter of the wire is known (0.68mm) and the length of wire used may be calculated. Using an average diameter for the primary winding of 1.275m the length of wire used was 6545m. Thus the resistance of the primary winding was calculated as 311 Ω. The measured values for the 3 coils 312 Ω, 316 Ω and 315 Ω.

The output resistor R_2 (Figure 5) dampens the LCR circuit and hence the value of R_2 should be chosen with care.

The relatively large diameter of the wire used in these ELF coils in addition to keeping the resistance of the primary winding low also lead to better defined problems for the calculation of the inductance and capacitance of these coils.

6. Inductance

The self inductance of the primary winding L_{11} is a measure of the magnetic flux linkage that the coil has with itself. The magnetic flux density, B, at any point due to the coil is the sum of the magnetic flux density caused by each individual winding at that point. For the purposes of determining the inductance only the component perpendicular to the plane of winding, B_Z, is significant. Working from Smythe's result [6] for the z component of the flux density due to a single coil, equation 9, the flux density at any point due to all the windings can be determined.

$$B_z(a,r,z)=\frac{\mu I}{2\pi}\ \frac{1}{r\left((a+r)^2+z^2\right)^{1/2}}\left(K+\frac{a^2+r^2+z^2}{(a-r)^2+z^2}\ E\right) \qquad (9)$$

Where a is the radius of the winding, K and E are the complete elliptical integral of the first and second kind respectively, z is the displacement along the z axis from the coil, and r is its radial displacement, μ is the permeability of the region and I is the current flowing in the winding.

Integrating numerically the flux Φ_m passing through winding m due to the current flowing in all the windings can be calculated by

$$\Phi_m=\sum_n\int_r B_z(a(n),\ r,\ z(n))\,2\pi r\,dr \qquad (10)$$

where n is the number of windings each with slightly different a and z value. The total flux passing through the coil Φ is the sum of the flux passing through each winding Φ_m. Thus the self inductance is

$$L_{11}=\sum_n \Phi_m \Big/ I. \qquad (11)$$

The mutual inductance between the primary winding and the excitation winding as well as the self inductance of the excitation winding were calculated using this method. These values were also measured at 20 Hz on a bridge. Care was taken while measuring the inductance of the ELF coils to place the coil under test away from ferrous and conducting materials, the results are shown in Table 1.

	Measured Inductance			Calculated Inductance
	Coil A	Coil B	Coil C	
Primary Winding	7.64 H	7.35 H	7.58 H	7.5 H
Excitation Winding	188 μH	188 μH	189 μH	180 μH
Primary - Excitation	27.5 mH	26.8 mH	27.4 mH	27.1 mH

Table 1 - ELF Coil Inductance

7. Capacitance

The capacitance C_2 in Figure 5 is the total of a number of separate capacitances. These include the capacitance of two cables, a junction box, the inter layer and inter slot capacitance of the primary winding and the stray capacitance between the excitation

and primary winding.

The capacitance of : - the 24 wire cable was 208 pF.
- the 8 wire cable was 145 pF.
- the junction box was 39 pF.
- the last junction box 20 pF.

These values were measured with only one ELF coil connected, as in test conditions, it is reasonable to believe they will increase slightly with all three ELF coils connected.

The capacitances of the three primary windings were measured as 156pF, 151pF and 154pF. As all three windings have similar capacitance despite the differences in their windings it suggests that an accurate prediction of their capacitance is possible.

When the construction of the ELF coils is examined it is apparent that there are three major sources of capacitance. These are due to the potential difference between the conductors:

- in the six slots.
- of the 34 layers in each slot.
- of the primary and excitation winding.

In order to calculate the capacitance of the coil, the windings will be modelled as parallel plates. In the following subsections such a model is developed.

7.1 Capacitance of Infinite Length Parallel Plates

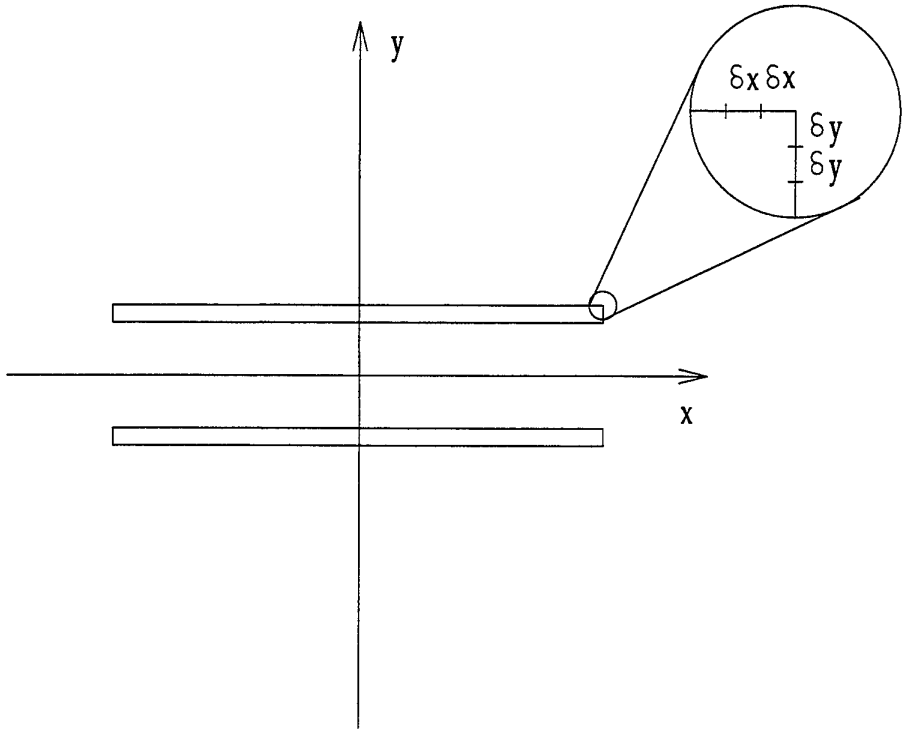

Figure 6 - Element alignment on Parallel Plate

In order to determine the capacitance of two parallel plates the surface of each plate was considered to consist of a finite number of elements. Each element is parallel to either the x or y axis with a length δx or δy respectively as shown in Figure 6. The potential and line charge density within each element is assumed to be uniform. The potential, V_p, at point p due to a infinite length line charge orientated parallel with the z axis is

$$V_p = \frac{-\sigma_l}{2\pi\varepsilon} Ln\left(x_1^{\,2} + y_1^{\,2}\right)^{1/2} \qquad (12)$$

where σ_l is the line charge density, ε is the permittivity, and (x_1, y_1) is the distance of the point from the infinite length line charge.

Each element consists of a number of line charges, all of which have the same line charge density and potential. The potential at the centre of element i due to the line charge densities of element j will be labelled V_{ij}. If the centre of element i is a distance (x_1, y_1) from the centre of element j the potential V_{ij} may be determined by

integrating equation 12 from $(x_1 - \delta x/2)$ to $(x_1 + \delta x/2)$ if the element is parallel to the X axis and from $(y_1 - \delta y/2)$ to $(y_1 + \delta y/2)$ if the element is parallel to the Y axis. Thus if the element j is parallel to the X axis

$$V_{ij} = \frac{-\sigma_l}{2\pi\varepsilon}\left[-2x + 2y_1 \tan^{-1}\left(\frac{x}{y_1}\right) + x\,Ln\left(x^2 + y_1^2\right)\right]_{x_b}^{x_a} = \sigma_l\, a_{ij} \qquad (13)$$

where $x_a = (x_1 + \delta x/2)$, $x_b = (x_1 - \delta x/2)$ and a_{ij} is a function of the inter element distance, the length, the orientation of the elements and a constant. When element j is parallel to the Y axis the variables x and y are swapped.

When considering the potential at an element due to itself $(x_1 + y_1 = 0)$ the distributed nature of the line charges within the element must be considered. Thus for an element parallel with the x axis

$$V_{ii} = -\frac{\sigma_l'}{2\pi\varepsilon}\int_{-\delta x/2}^{\delta x/2} \ln x\, dx = -\frac{\sigma_l}{2\pi\varepsilon}\left(\ln\left(\frac{\delta x}{2}\right) - 1\right) = \sigma_l\, a_{ii} \qquad (14)$$

where $\sigma' = \sigma/\delta x$. The potential at an element will be the sum of the contributions from all the elements shown in Figure 6. Thus the potential at (the centre of) one of the elements is the sum of the contributions from the line charges of all elements. Thus the potential, V_i, at the centre of element i in a system of n elements is

$$V_i = \sum_{j=1}^{n} a_{ij}\sigma_{lj} \qquad (15)$$

where σ_{lj} is the line charge density of element j and a_{ij} is determined as shown in equation 13 and 14. When equation 15 is applied to all elements a matrix as shown in *Table* 2 is created.

$$\begin{vmatrix} V_1 \\ V_2 \\ .. \\ .. \\ .. \\ .. \\ V_i \end{vmatrix} = \begin{vmatrix} a_{11}\ a_{12}\ ..\ ..\ ..\ ..\ ..\ a_{1j} \\ a_{21}\ ..\ ..\ ..\ ..\ ..\ ..\ ..\ .. \\ .. \\ .. \\ .. \\ .. \\ a_{i1}\ ..\ ..\ ..\ ..\ ..\ ..\ a_{ij} \end{vmatrix} \begin{vmatrix} \sigma_{l1} \\ \sigma_{l2} \\ .. \\ .. \\ .. \\ .. \\ \sigma_{lj} \end{vmatrix}$$

Table 2 - Matrix for calculating line charge density

where $i = j = n$, the number of elements.

In order to determine the capacitance of the two plates a potential difference of V is applied between the plates. As the total charge on each plate has the same absolute value the potential of one plate is set at V/2 and the other at -V/2, ie each plate contributes equally to the over all capacitance. As the potential of all elements is known the matrix may be solved and the line charge density σ_{ij} of each element thus determined.

Once the line charge density of each element has been determined the energy E stored in the capacitor may be calculated.

$$E = \frac{1}{2}\sum_{i=1}^{n} \sigma_{li} V_i \qquad (16)$$

The capacitance C between the two plates is

$$C = {}^{2E}/_{V^2} \qquad (17)$$

When the value of the line charges is examined it is apparent that for two parallel plates each at a constant potential the magnitude of the line charges is symmetrical about the x and y axis of the capacitor. This would be expected from the initial formulation of the problem. Using this knowledge the dimensions of the matrix may be reduced by a factor of four so long as the coefficient a_{ij} is modified to include the influence of the additional 3 elements. The results for different widths w to separation distances d for extremely thin parallel plates are displayed in Figure 7 along with the results obtained when fringe effects are ignored. The capacitance per unit length C_∞ when fringe effects are ignored were determined from equation 18.

$$C_\infty = {}^{\varepsilon w}/_{d} \qquad (18)$$

From Figure 7 it is apparent that as the ratio of conductor width to separation distance increases the results obtained by the parallel plate method approach the results from the method that neglects fringe effects.

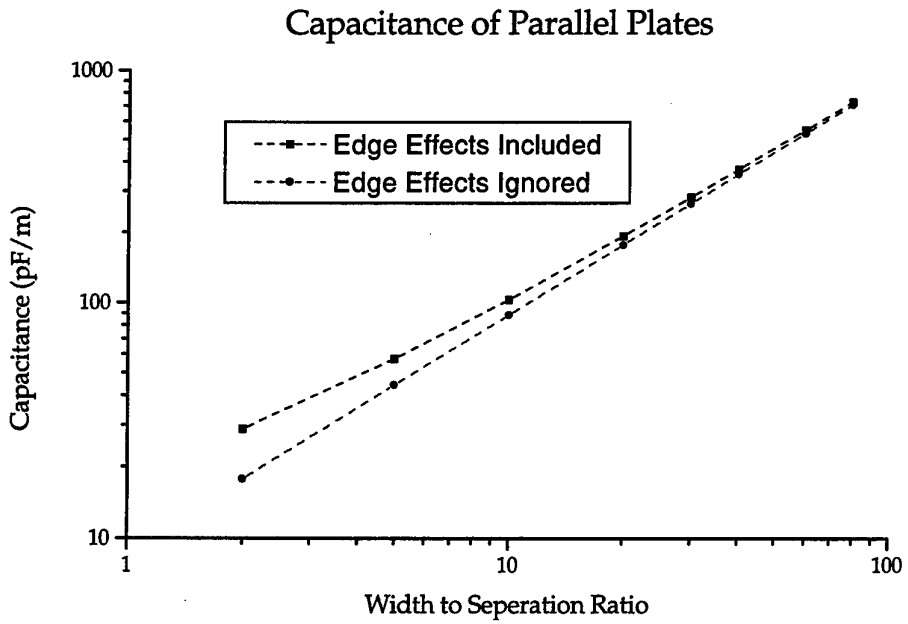

Figure 7 - Calculated Capacitance of Parallel Plate

The method used to calculate the capacitances of two parallel plates was then expanded to calculate the capacitances of systems with many parallel plates where symmetry existed in the reflection through the x axis. The symmetry conditions require that the plate at y matches an identical plate at $-y$ and the average potential of the plate at y has the opposite average potential of the plate at $-y$, ie each plate in that pair contributes equally to the capacitance.

Consider two parallel plates a distance apart at a fixed potential V/2 (top) and –V/2 (bottom). The potential in the space between these two plates will be vary linearly between the top plate where the potential is V/2 and the bottom plate where the potential is –V/2. If another plate is inserted between the top and bottom plate the amount of change on the plate will depend on the potential of the new plate and the potential that would be at the location of the new plate due to the plates that are already there. If the potential of the new plate is the same as the potential that already existed at the location before the new plate was inserted no charge will reside on the new plate.

7.2 Application of the Infinite Length Parallel Plate Method to the ELF Coils

A method to calculate the capacitance between two concentric rings of finite width may be applied to a problem involving finite width parallel plates of infinite length by allowing the diameter of these rings to approach infinity. Conversely if the inside diameter of two concentric rings greatly exceeds their thickness the infinite length parallel plate model can be applied to calculate the capacitance between the rings. This criterion is meet by the ELF coils used by MEDAS.

7.2.1 Inter Slot Capacitance

In the initial calculations of the inter slot capacitance each slot was treated as a conductor at a constant potential. This appeared to be a valid approximation as there is a constant potential difference V_{is} between the slots in the radial and tangential directions.

$$V_{is} = \frac{N_s - 1}{N_s} V_{pri} \qquad (19)$$

where V_{pri} is the potential induced in the coil and N_s is the number of slots. The potential difference between the top and bottom of each slot is V_{pri}/N_s if the earth is connected to the beginning of the primary winding and $-V_{pri}/N_s$ if earth is connected to the end of the winding.

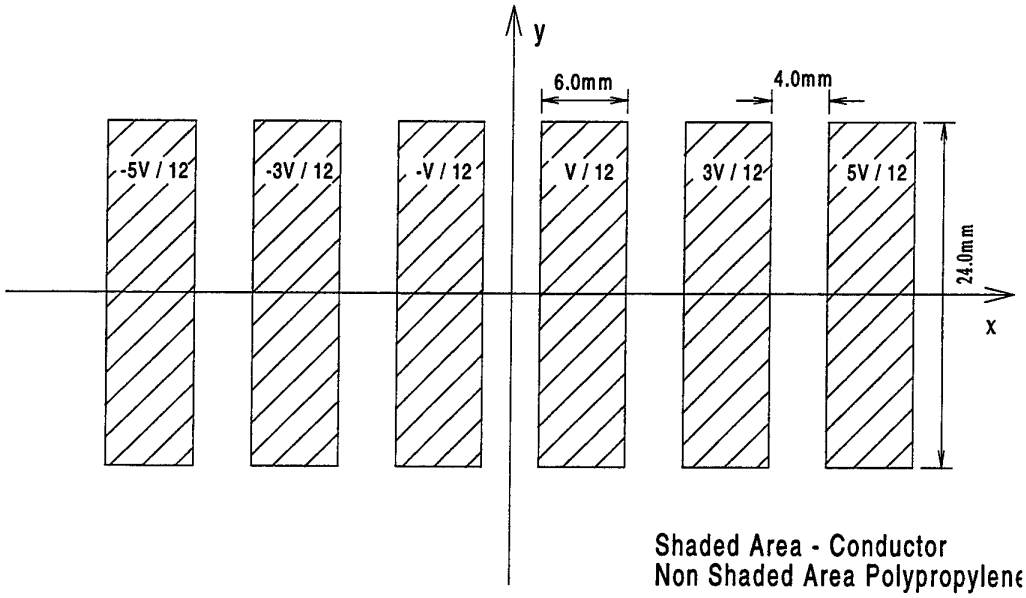

Figure 8 - Formulation of inter slot capacitance problem

The construction of the ELF coils used in this analysis is shown in Figure 1 and the earth was connected to the beginning of the primary coil. Figure 8 shows the formulation of this problem. The infinite length parallel plate method was used to calculate the line charge density of each element and thus the capacitance. The sum of the line charge density for each slot is shown in table 3.

Slot	Sum of Line Charge Density
1	3.764×10^{-11} C/m
2	3.773×10^{-12} C/m
3	1.085×10^{-12} C/m
4	-1.085×10^{-12} C/m
5	-3.773×10^{-12} C/m
6	-3.764×10^{-11} C/m

Table 3 - Sum of line charge density for uniform potential difference

From the potential and the total line charge density of each slot the capacitance was calculated as 33.5 pF/m using equations 16 and 17. As the average diameter of the coil is 1.275m the over all inter slot capacitance was 134 pF.

This model was then further developed to allow for the potential varying with the

radial distance. This was achieved by allowing the potential of each element on a plate to vary depending on its radial displacement. The sum of the line charge densities of each slot calculated using this method are shown in table 4.

Slot	Sum of Line Charge Density
1	3.765×10^{-11} C/m
2	3.773×10^{-12} C/m
3	1.084×10^{-12} C/m
4	-1.084×10^{-12} C/m
5	-3.773×10^{-12} C/m
6	-3.765×10^{-11} C/m

Table 4 - Sum of line charge density for radial varying potential difference

From the potential and the line charge density of each element the capacitance was calculated as 35.3 pF/m using equations 16 and 17. The overall inter slot capacitance was calculated 141 pF.

It thus appears that the approximation, used in calculating table 3, of treating each slot as a plate at a constant potential was reasonable. This approximation is valid only as there is a constant potential difference between each slot in the radial and tangential direction. In both results the majority of the charge resided on the inside surface of the external plates.

7.2.2 Inter Layer Capacitance

The inter layer capacitance is the capacitance of each slot due to the difference in potential of the layers within the slot. The potential difference between the beginning of first winding and the end of the last winding in any slot is V_{pri}/N_s. In this calculation there is not a constant potential difference in the axial direction, only the tangential direction, so each turn will be considered as a separate element at a known potential. The potential difference in the axial direction is not constant as if a layer is wound from left to right the layer above this will be wound from right to left. The potential of an element will depend on its position.

When the infinite length parallel plate method was adapted and applied to the inter layer capacitance as shown in Figure 9 the capacitance was calculated as $41\varepsilon_r$ pF/m.

Thus the inter layer capacitance for each slot is $166\varepsilon_r$ pF. The relative permittivity ε_r of the gap between the conducting plates was determined from the cross sectional area in each slot of plastic (wire insulation ester imide) and air. The ratio of the wire insulation to air was calculated as 1:1.8, the relative permittivity ε_r of the insulation was approximately 2.5, thus the value of ε_r in the gap between conducting layers was taken as 1.54. When the six of the inter layer capacitance are added in series the contribution of the inter layer capacitance to the overall capacitance is 43pF. This value is only approximate due to uncertainties in the calculation of ε_r and the small distance between layers.

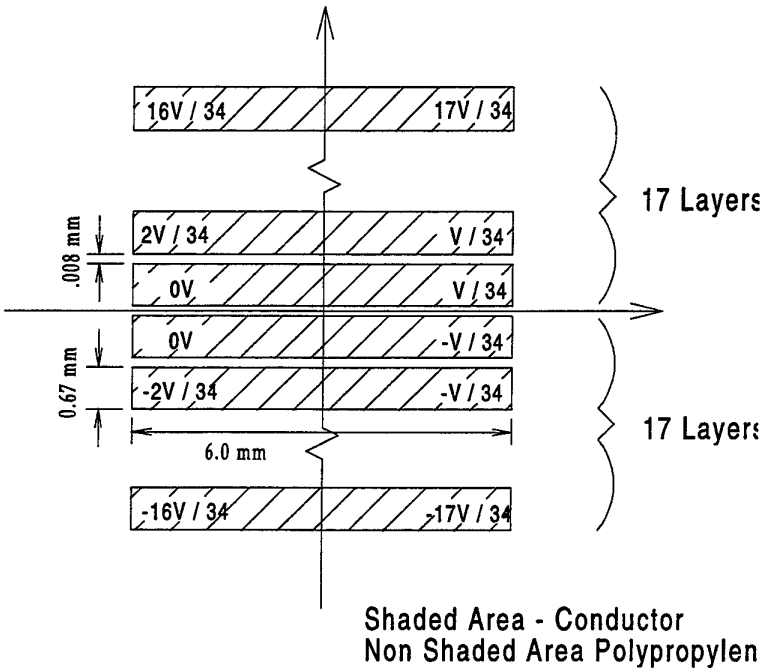

Figure 9 - Formulation of inter layer capacitance

7.2.3 Inter winding Capacitance

The infinite length parallel plate method was used to calculate the capacitance between the six turns of the excitation winding and the eight turns of the primary winding directly above it. A strip of mylar 0.06 mm thick was placed between the two layers, allowing for this and the relative permittivity of the rest of the gap between layers determined in section 7.2.2, the average permittivity was estimated as 1.8. A constant potential was assumed on each plate. The capacitance was calculated as 545pF/m or 2.13nF for the total inter winding capacitance. The diameter of the excitation winding

is 1.25m. An important consideration for the performance of the coil is the potential difference, V_{iw}, across this capacitance. This potential difference depends where the excitation winding is placed and is further discussed in section 9. The excitation winding was placed at the bottom of the sixth slot in the ELF coil used in this analysis. Thus the potential difference V_{iw} across this capacitance is $V_{pri}/6$. The contribution of this to the overall capacitance is

$$C_{iw} = \left(\frac{1}{6}\right)^2 \times 2.13\ nF = 59\ pF \qquad (20)$$

This value is only a rough estimation and varies considerable depending how the two layers in question are wound. The values measured for the inter winding capacitance were 2.66nF, 2.02nF and 2.56nF.

7.3 Summary of Capacitances

The calculated and measured values for the capacitances are summarised in table 5.

Capacitance	Coil Measured			Calculated Value
	Coil A	Coil B	Coil C	
Inter Slot	⎫	⎫	⎫	141 pF⎫
	⎬ 156 pF	⎬ 156 pF	⎬ 151 pF	⎬ 183 pF
Inter Layer	⎭	⎭	⎭	43 pF ⎭
Inter Winding	74 pF	56 pF	71 pF	59 pF

Table 5 - Summary of measured and calculated capacitance values

For the purposes of calculation the inter slot capacitance is the best defined. The polypropylene wall separating the conductors provides a gap so that the distance between the conductors is constrained and the dielectric constant is almost constant.
The distance between the conductors that produce the inter layer capacitance is determined from the thickness of the insulation. The value of the permittivity was estimated from the ratio of air to dielectric. For this calculation to be valid care must be taken in applying the correct tension to the wire when it is placed on the former. This enables the layers to sit on top of each other. Minor inconsistencies should average out.
The calculation of the inter winding capacitance is poorly defined. The positioning of the 6 turns within a slot is not tightly constrained and there are not enough turns to

average out small inconsistencies. The value calculated for the inter winding capacitance is only a "ball park" figure. This should not matter however as by correctly positioning the excitation winding the effect of this capacitance on normal operation may be removed, this is discussed in section 9.

8. Excitation Winding

The excitation winding is used to produce a magnetic field to enable the function of the primary winding and associated electronics to be tested when the device is underwater. Figure 3 displays the frequency response of the primary winding when excited by the excitation winding.
The potential induced across the primary winding V_{pri} by a current i_e in the excitation winding can be calculated using equation 21.

$$V_{pri} = L_{12}\frac{di_e}{dt} \qquad (21)$$

The values obtained for the mutual inductance L12 between the primary and excitation winding are given in section 6. When the excitation winding is used to excite the primary winding a slight difference in the frequency response of the primary winding is apparent, this may be seen in Figure 4. The simple circuit model depicted in Figure 5 does not explain this difference.

9. Discussion

With ELF coils a major constraint on their possible sensitivity will be limitations on their size and weight. Given a required sensitivity over a frequency bandwidth and a limitation on their size and thus their area, equation 4 may be used to determine the number of turns required on the primary winding.

The resistance R_1 of the primary winding may then be determined from the diameter of the former, the number of turns and the gauge of wire used. The gauge of wire used will also influence the calculations of the capacitance and inductance.

The inductance L_{11} and the contribution to the capacitance C_2 from the ELF coil

may be determined from sections 6 and 7 respectively. The capacitance C_2 will also be increased if cabling is placed onto the output of the primary windings before the amplifier. The resistance R_2 is the input resistance of the amplifier, this resistor has a major influence on the frequency response of the coil as it dampens the LC circuit formed by the primary winding. Once the value of these components is known equations 7 and 8 may be used to examine the behaviour of the ELF coils. If the resonance frequency occurs within or close to the required bandwidth it may be desirable to alter the design. (Alternately the resonance point may be chosen to amplify some frequencies.)

The value of C_2 calculated from the resonance frequency of the ELF coils is 720pF. As the capacitance of the coil without the cabling is approximately 230pF the magnitude added to C_2 due to the cabling and junction boxes is approximately 490pF. The increase in C_2 determined from the measured values of the cabling and junction boxes was 412pF. Unfortunately when this discrepancy was noted the cabling was no longer available for testing. Using the 490pF value for the cabling capacitances and the calculated values of the inter slot, inter layer and inter winding capacitance, the calculated value of C_2 is 732pF. Using equations 4 and 7 the predicted frequency response of the coils may be calculated, the predicted and measured frequency response are compared in Figure 10.

Looking at the design of the ELF coils used in this analysis the most obvious way of increasing the resonance frequency without altering the sensitivity would be to reduce the capacitance C_2. A reduction in C_2 can be achieved by placing the amplifier before the cabling. Doing this for the coil used in this analysis would reduce the expected capacitance from 720pF to 230pF, thus increasing the resonance frequency by a factor of 1.8.

A possible cause of C_2 becoming large is a poorly positioned excitation winding. For maximum magnetic coupling the excitation winding would be placed in one of the centre slots. It is more important however to place the excitation winding to minimise the contribution of the inter winding capacitance to the total capacitance. This is achieved by minimising the potential difference across this capacitance. Thus ideally it would be placed next to the layer of the primary winding that is earthed so in normal operation (excitation winding grounded) it would have no effect. The ELF coil used in this analysis had its excitation winding placed on the bottom of the sixth slot so $V_{iw} = V_{pri}/6$.

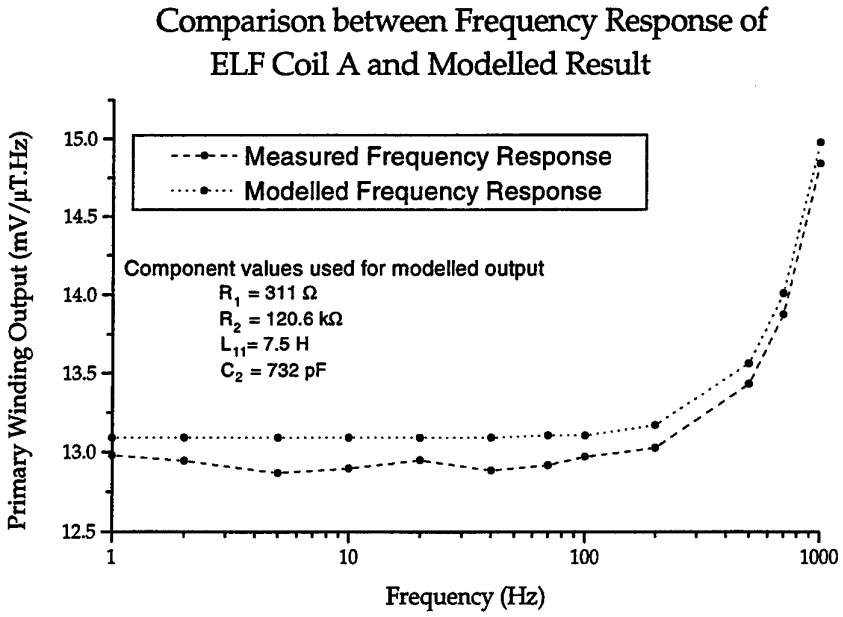

Figure 10 - Modelled and measured outputs of the primary winding

If the excitation winding had been placed at the bottom of the first slot however V_{iw} would have been V_{pri} and the contribution to the total capacitance would have been increased by a factor of thirty six. Such a capacitance would drastically reduce the resonance frequency. (In the case where the excitation winding is in the first slot by changing the end of the primary winding earthed the potential across the inter winding capacitance could be reduced for all practical purposes to zero. Thus removing the influence of the inter winding capacitance.) Using equation 4 and 7 the expected frequency response of these ELF coils without the additional capacitance due to cabling and the inter winding capacitance may be determined. Figure 11 shows the expected frequency response of the ELF coils using the measured and calculated values for L_{11}, R_1 and C_2 where C_2 is without the additional capacitance due to the cabling and inter winding capacitance. The values used for L_{11}, R_1, C_2 and R_2 are shown in table 6.

	Measured Value	Calculated Value
R_1	312 Ω	311 Ω
R_2	120.6 kΩ	
L_{11}	7.5 H	7.64 H
C_2	155 pF	183 pF

Table 6 - Measured and calculated values used in Figure 11

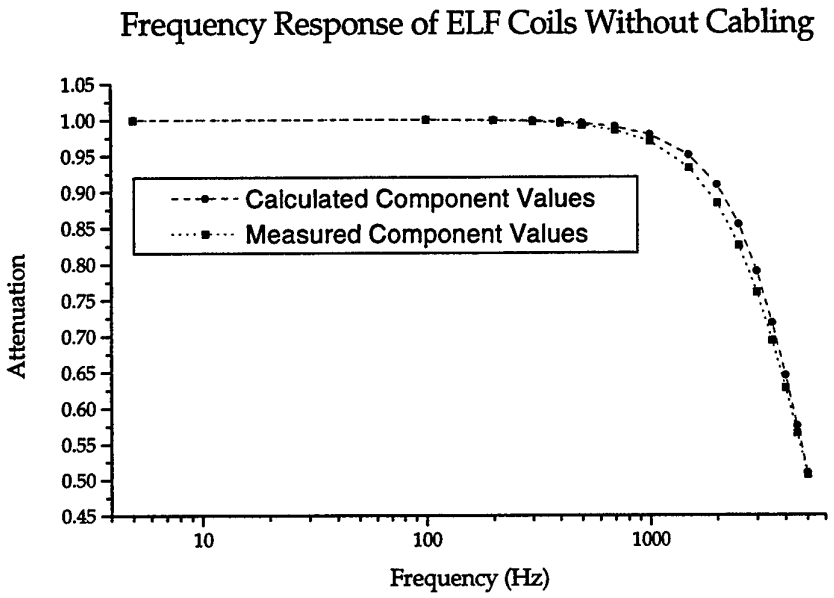

Figure 11 - Modelled output of the primary winding using measured and calculated component values in the circuit model

10. Conclusion

A vessel's ELF signature can be extracted from the output of the MEDAS ELF coils primary winding using the frequency response shown in Figure 2. The frequency response is a function of the capacitances, inductances and resistances in the ELF coil and its associated circuitry. For the ELF coils used in MEDAS the sensitivity of the coils

was approximately 12.9 mV/(μT.Hz) up to 100 Hz, increasing to around 13.6 mV/(μT.Hz) at 600 Hz.

Once the origin of the capacitances in the ELF coil were identified methods were developed to calculate the magnitude of these capacitances. The self and mutual inductance along with the resistance of the windings in the coil were also calculated. These calculated values are used in equation 7 and 8 to determine the frequency response of the ELF coils.

The majority (70%) of the capacitances present in the system is due to cabling and junction boxes attached to the coils before the amplifiers. Placing the amplifiers before the cabling will prevent the capacitances of the cables from altering the resonance frequency. Possible problems caused by poor placement of the excitation winding or incorrect earthing of the primary coil were also identified. With these minor changes the resonance frequency of the primary winding could be approximately doubled thus providing a straighter frequency response for future ELF coils.

11. Acknowledgments

The winding layout for these coils was copied from coils made by Dr Julian Vrbancich, Maritime Operations Division[2] (MOD). The construction technique used for these ELF coils were developed by Max Coxhead, MOD. The ELF coils used during this project were constructed by the Aeronautical and Maritime Research Laboratory[3] workshop. The MEDAS project was managed by Peter Ramsay (retired), MOD.

The author wishes to thank Dr John Ternan (retired), MOD for his assistance though out this project. Dr John Ternan designed the Magnetic Test Facility used to test the ELF coils. The construction of this facility was overseen by Jack Wilson MOD and the late Jim McBeath, MOD.

12. References

1. Vrbancich, J. and Scott, L. (1993)

[2] Underwater Systems Division at the time this work was performed
[3] Materials Research Laboratory at the time this work was performed

Extremely Low Frequency magnetic and electric fields from navel vessels.
MRL Technical Report MRL-TR-92-45.

2. Vrbancich, J., Turnbull, S. and Scott, L. (1993)
An underwater Extremly Low Frequency (ELF) Magnetic and electric field detection system.
MRL Research Report MRL-RR-5-93

3. Vrbancich, J. (1987)
Air-Core Induction Coils : Alternating Magnetic Field Sensors
MSD Technical Note 4/87. Sydney, N.S.W. Weapons System Research Laboratory.

4 Holtham, P.M. (1983)
New High Frequency Electromagnetic Detection System.
Technical Memorandum 83-9, Defence Research Establishment Pacific, Esquimalt, Victoria
Canada.

5 Wesley, V. F. (1950)
The Theory of Induction Coils.
Macdonald, London.

6 Smythe, W.R. (1950)
Static and dynamic electricity, 2nd., pp.270-271. New York:
McGraw Hill Book company Inc.

DISTRIBUTION LIST

Extra Low Frequency (ELF) Coils for the Marine Environment Data Acquisition System (MEDAS)

David Clarke

AUSTRALIA

DEFENCE ORGANISATION

Task Sponsor **DMCD**

S&T Program

Chief Defence Scientist
FAS Science Policy
AS Science Corporate Management
} shared copy

Director General Science Policy Development
Counsellor Defence Science, London (Doc Data Sheet)
Counsellor Defence Science, Washington (Doc Data Sheet)
Scientific Adviser to MRDC Thailand (Doc Data Sheet)
Scientific Adviser Policy and Command
Navy Scientific Adviser
Scientific Adviser - Army (Doc Data Sheet and distribution list only)
Air Force Scientific Adviser
Director Trials

Aeronautical and Maritime Research Laboratory

Director
Chief of Maritime Operations Division
Dr A Theobald
Frank May
Dr Julian Vrbancich
David Clarke

DSTO Library and Archives

Library Fishermans Bend
Library Maribyrnong
Library Salisbury (2 copies)
Australian Archives
Library, MOD, Pyrmont
Library, MOD, HMAS Stirling
US Defense Technical Information Center, 2 copies
UK Defence Research Information Centre, 2 copies
Canada Defence Scientific Information Service, 1 copy
NZ Defence Information Centre, 1 copy
National Library of Australia, 1 copy

Capability Development Division

Director General Maritime Development
Director General Land Development (Doc Data Sheet only)

Director General C3I Development (Doc Data Sheet only)
Director General Aerospace Development (Doc Data Sheet only)

Navy

SO (Science), Director of Naval Warfare, Maritime Headquarters Annex, Garden Island, NSW 2000. (Doc Data Sheet only)

Army

ABCA Standardisation Officer, Puckapunyal, (4 copies)
SO (Science), DJFHQ(L), MILPO Enoggera, Queensland 4051 (Doc Data Sheet only)
NAPOC QWG Engineer NBCD c/- DENGRS-A, HQ Engineer Centre Liverpool Military Area, NSW 2174 (Doc Data Sheet only)

Intelligence Program

DGSTA Defence Intelligence Organisation
Manager, Information Centre, Defence Intelligence Organisation

Corporate Support Program

OIC TRS, Defence Regional Library, Canberra

UNIVERSITIES AND COLLEGES

Australian Defence Force Academy
Library
Head of Aerospace and Mechanical Engineering
Serials Section (M list), Deakin University Library
Senior Librarian, Hargrave Library, Monash University
Librarian, Flinders University

OTHER ORGANISATIONS

NASA (Canberra)
Info Australia (formerly AGPS)

OUTSIDE AUSTRALIA

ABSTRACTING AND INFORMATION ORGANISATIONS

Library, Chemical Abstracts Reference Service
Engineering Societies Library, US
Materials Information, Cambridge Scientific Abstracts, US
Documents Librarian, The Center for Research Libraries, US

INFORMATION EXCHANGE AGREEMENT PARTNERS

Acquisitions Unit, Science Reference and Information Service, UK
Library - Exchange Desk, National Institute of Standards and Technology, US

SPARES (5 copies) **Total number of copies:** 54

DEFENCE SCIENCE AND TECHNOLOGY ORGANISATION
DOCUMENT CONTROL DATA

1. PRIVACY MARKING/CAVEAT (OF DOCUMENT)

2. TITLE

Extra Low Frequency(ELF) Coils for the Marine Environment Data Acquisition System (MEDAS)

3. SECURITY CLASSIFICATION (FOR UNCLASSIFIED REPORTS THAT ARE LIMITED RELEASE USE (L) NEXT TO DOCUMENT CLASSIFICATION)

Document	(U)
Title	(U)
Abstract	(U)

4. AUTHOR(S)

David Clarke

5. CORPORATE AUTHOR

Aeronautical and Maritime Research Laboratory
PO Box 4331
Melbourne Vic 3001 Australia

6a. DSTO NUMBER	6b. AR NUMBER	6c. TYPE OF REPORT	7. DOCUMENT DATE
DSTO-TR-0876	AR-011-084	Technical Report	September 1999

8. FILE NUMBER	9. TASK NUMBER	10. TASK SPONSOR	11. NO. OF PAGES	12. NO. OF REFERENCES
510/207/0945	NAV 93/226	DMCD	28	6

13. INTERNET ADDRESS (URL) OF PDF VERSION

http://www.dsto.defence.gov.au/corporate/reports/DSTO-TR-0876.pdf

14. RELEASE AUTHORITY

Chief, Maritime Operations Division

15. SECONDARY RELEASE STATEMENT OF THIS DOCUMENT

Approved for public release

OVERSEAS ENQUIRIES OUTSIDE STATED LIMITATIONS SHOULD BE REFERRED THROUGH DOCUMENT EXCHANGE, PO BOX 1500, SALISBURY, SA 5108

16. DELIBERATE ANNOUNCEMENT

No Limitations

17. CASUAL ANNOUNCEMENT Yes

18. DEFTEST DESCRIPTORS

ELF, Electromagnetic inductance, magnetic signatures, signatures

19. ABSTRACT

Three Extra Low Frequency (ELF) coils for measuring low frequency magnetic signatures were designed and built for use with the Marine Environment Data Acquisition System (MEDAS) concept demonstrator. This report details the tests conducted to determine the performance of these coils. A circuit model of the ELF coils is developed so the output of the coils may be related to the incident magnetic field. The values for the resistance, inductance and capacitance are measured and calculated from details of the construction. The effect of incorporating a calibration winding for checking the in-situ underwater response of the ELF coils are also examined.